

Diffuse and weak Bragg scattering from quasicrystals: pitfalls and opportunities

Thomas Weber* and Walter Steurer

Laboratory of Crystallography, Department of Materials, Wolfgang-Pauli-Strasse 10, 8093 Zurich, Switzerland

Received July 21, 2008; accepted August 18, 2008

Quasicrystals / Diffuse scattering / Disorder / Experimental artefacts

Abstract. The influence of limited experimental reciprocal space resolution on the appearance of diffraction patterns from quasicrystals is discussed. Using simulated data from a perfectly ordered one-dimensional Fibonacci chain it is shown that realistic experimental resolution effects may lead to artificial ‘diffuse scattering’ of significant intensity. Two different diffuse features are identified in simulations of macroscopically sized crystals. A broad and almost smooth diffuse background is found, which strongly increases with decreasing reciprocal space resolution. In addition, a set of narrow diffuse peaks having profiles similar to thermal and phasonic diffuse scattering is present, which is only seen in high resolution patterns. The former diffuse scattering represents unresolved Bragg reflections, while the latter is due to truncation effects coming from the finite crystal size. The relevance of the findings for the understanding of real experimental diffraction patterns is discussed on the examples of diffuse scattering from $d\text{-Al}_{70}\text{Co}_{12}\text{Ni}_{18}$ and $i\text{-Al}_{64}\text{Cu}_{23}\text{Fe}_{13}$. Finally, some criteria for distinguishing disorder diffuse scattering from artificial diffuse scattering are given.

1. Introduction

By definition, disorder is any local deviation from (possibly higher-dimensional) perfect translation periodicity. In scattering experiments, it is identified by the presence of diffuse scattering in addition to sharp Bragg reflections. For periodic structures, the reverse conclusion is true as well: observation of non-parasitic diffuse scattering is a proof for the presence of disorder¹. But is this also true for quasicrystals, where Bragg reflections may get arbitrarily close in parallel space? Do reflections show a continuous ‘diffuse’ pattern, if they cannot be resolved experimentally? Theory says that Bragg reflections having a short separation in parallel space are widely separated in

perpendicular space and therefore corresponding intensities are expected to differ strongly; otherwise a discrete set of sharp Bragg reflections would not be visible. It is usually assumed that Bragg reflections having very high perpendicular space components are too weak to be observed as individual peaks, but their total contribution to an experimental diffraction pattern has not been investigated so far. The question about the appearance of weak Bragg reflections as discrete or continuous phenomena in diffraction experiments is of particular importance when searching for energy-stabilized, perfect quasicrystals, *i.e.* quasicrystals with negligible entropy contribution.

In the first part of this paper, we will discuss the expected experimental diffraction pattern from a perfect quasicrystal by means of computer simulations. The focus will be on the influence of limited experimental resolution on the appearance of weak diffraction features. The second part will show how disorder diffuse scattering in real examples can be distinguished from artificial diffuse scattering coming from resolution effects.

2. ‘Diffuse scattering’ from a perfect quasicrystal

If interested in weak diffraction phenomena higher dimensional (nD) modelling provides an incomplete representation of parallel space diffraction intensities, because it is not possible to fully consider all diffraction intensities along perpendicular space directions. This is in contrast to experiments, which implicitly provide a full integration of the perpendicular reciprocal space. To be as close as possible to diffraction experiments the simulations shown in this paper were exclusively performed in physical space. The calculations are based on a one-dimensional (1D) Fibonacci chain (FC) built of 10000 Al atoms, which are separated by $S = 2.40 \text{ \AA}$ and $L = \tau \times 2.40 \text{ \AA} \approx 3.88 \text{ \AA}$. The resulting model has a length of $\sim 3.32 \mu\text{m}$, *i.e.* it is a crystal of macroscopic size. The calculated intensities represent the squared modulo of the Fourier transform of the complete structure. The step width in reciprocal space is $5 \times 10^{-6} \text{ \AA}^{-1}$ which fulfils Shannon’s sampling criterion ($\Delta h \leq 1/(2 \times 3.32 \mu\text{m}) \approx 1.5 \times 10^{-5} \text{ \AA}^{-1}$) for a lossless representation of the diffraction data (note that reciprocal space units are defined as $h = 1/d = 2 \sin \theta/\lambda$). The calcu-

* Correspondence author (e-mail: thomas.weber@mat.ethz.ch)

¹ Incommensurately modulated crystals and periodic crystals with unit cells larger than the coherence length of the experiment are special cases, which are not considered.

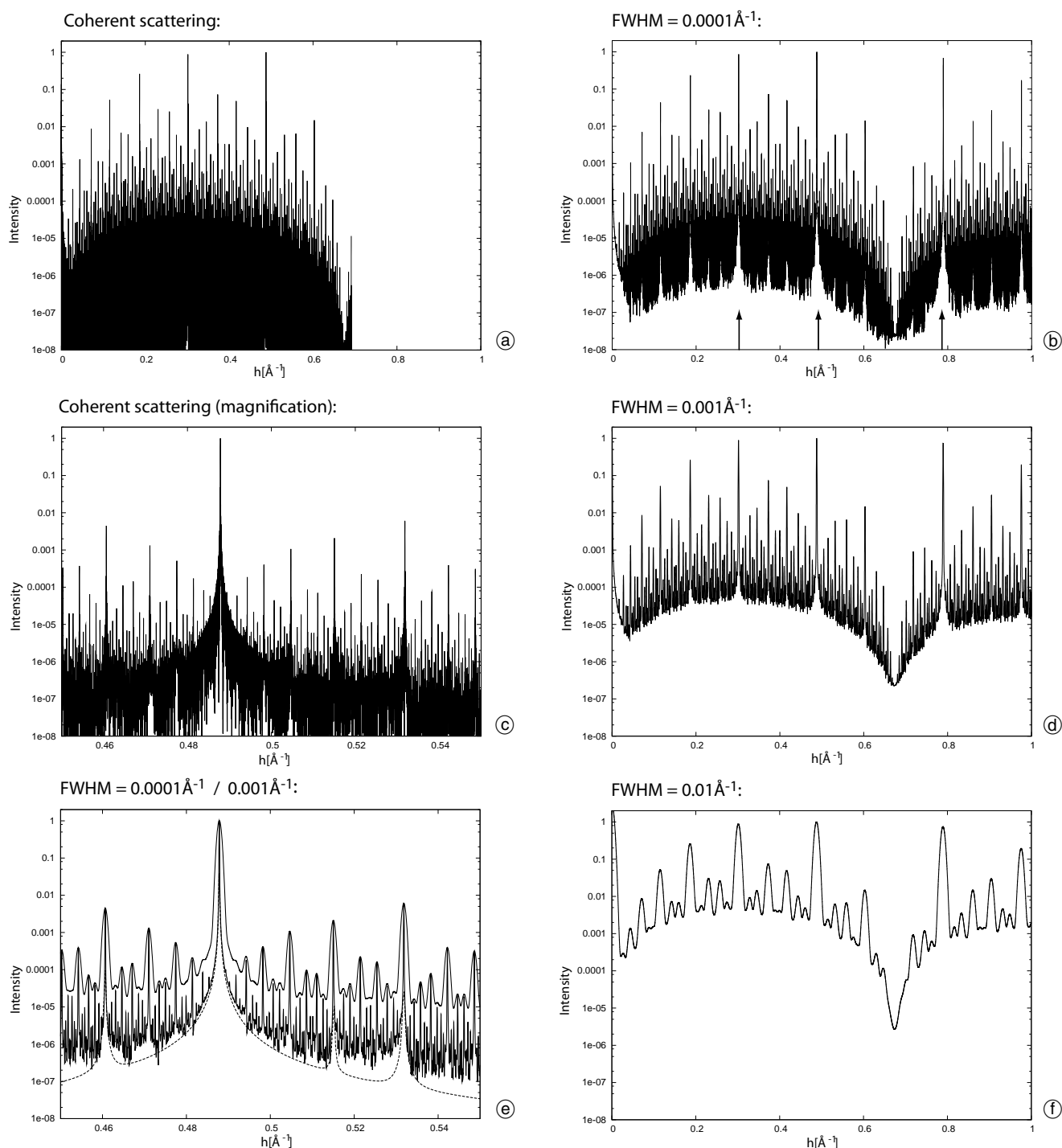


Fig. 1. Computer simulations of diffraction patterns of a perfect FC. Intensities are normalized to the strongest intensity except $I(0)$ in the respective pattern. All patterns are plotted on a logarithmic scale with a dynamic range of 10^8 . Patterns (a) and (c) show the fully coherent diffraction intensities, (b), (d) and (f) show the effect of resolution functions with $\text{FWHM} = 0.0001 \text{ \AA}^{-1}$, 0.00 \AA^{-1} and 0.01 \AA^{-1} , respectively. The arrows in (b) indicate some of the narrow diffuse features coming from truncation effects. Zoomed sections of (b) and (d) are shown in (e). The dashed line in (e) indicates the $1/q^2$ decay of the diffuse background relative to strong reflections. The $1/q^2$ decay model is a good description for the high resolution pattern with a resolution function of $\text{FWHM} = 0.0001 \text{ \AA}^{-1}$, but not for $\text{FWHM} = 0.001 \text{ \AA}^{-1}$.

lated diffraction pattern of the ideal FC (Figs. 1a, c) is thus fully coherent, complete (except for the finite reciprocal space extension and missing diffraction phases) and error free (*i.e.* without noise due to counting statistic, background, *etc.*). As expected from theory, a dense set of Bragg reflections covering a broad dynamic range of intensities is visible. Experimental limitations, however, do not allow measuring diffraction intensities as precisely as they may be calculated in computer simulations. To simu-

late resolution effects, the coherent diffraction patterns shown in Figs. 1a, c were convoluted with Gaussians of variable widths. The full widths at half maxima (FWHM) of the resolution functions used in the computer experiments were selected such that they cover the full range typically accessible in diffraction experiments. Three scenarios are compared: (i) high resolution synchrotron radiation in combination with a point detector were simulated by using a resolution function with $\text{FWHM} = 0.0001 \text{ \AA}^{-1}$,

(ii) synchrotron radiation experiments in combination with an area detector were imitated with a resolution function of half-width 0.001 \AA^{-1} and (iii) low resolution in-house or neutron experiments were simulated using a resolution function with $\text{FWHM} = 0.01 \text{ \AA}^{-1}$. As expected, the resulting diffraction patterns (Figs. 1b,d,f) become smoother compared to the fully resolved pattern and they show less, but broader Bragg reflections. In addition, a more or less continuous diffuse background is visible coming from unresolved weak Bragg reflections with high perpendicular space components. In scenario (i) the maximum diffuse intensity is about 4×10^{-7} times the maximum Bragg intensity, *i.e.* an intensity that is hardly visible. The ratio $I_{\text{diffuse}}^{\text{max}}/I_{\text{Bragg}}^{\text{max}}$ strongly increases with increasing width of the resolution function. For the case (ii) diffuse scattering is already of significant intensity ($I_{\text{diffuse}}^{\text{max}}/I_{\text{Bragg}}^{\text{max}} = 4 \times 10^{-5}$) and for case (iii) the ratio $I_{\text{diffuse}}^{\text{max}}/I_{\text{Bragg}}^{\text{max}} = 4 \times 10^{-3}$ can be considered as representing strong diffuse scattering. In all cases, the Bragg reflections still form a dense set and the shortest separation between Bragg reflections is about twice the half-width of the resolution function. In contrast to the maximum intensity of the diffuse background, which increases quadratically with an increasing width of the resolution function, the integral diffuse scattering shows a linear dependency on the width of the resolution function. The following ratios were obtained by interpolation of the broad diffuse background and subsequent numerical integration: $I_{\text{diffuse}}^{\text{integral}}/I_{\text{Bragg}}^{\text{integral}} = 3 \times 10^{-4}$ for case (i), 3×10^{-3} for case (ii) and 3×10^{-2} for scenario (iii).

In addition to the broad diffuse background, some relatively narrow diffuse peaks, having their maxima beneath the strongest reflections are observable (see arrows in Fig. 1b). In contrast to the broad diffuse background discussed above the narrow peaks become less visible with decreasing resolution. Simulations with variable crystal size indicate that the diffuse maxima are not coming from unresolved Bragg peaks, but they are representing truncation effects due to the finite crystal size. Although a crystal of macroscopic size was used, the truncation effects shown in Fig. 1b are strong enough to be detected in an experiment. In the high resolution case the intensity of the diffuse peaks decays with $1/q^2$, where q is the distance from the Bragg positions (Fig. 1e). This is a typical behaviour for thermal and phason diffuse scattering (TDS and PDS) and may therefore be misinterpreted accordingly. In practice, however, distinguishing truncation effects from TDS/PDS is not a problem. The intensity of truncation effects is in a good approximation proportional to the corresponding Bragg peak, while TDS/PDS is in addition affected by the external and internal space component of the associated Bragg reflection. Furthermore, the shape of diffuse truncation effects beneath Bragg reflections does not change at different reciprocal space positions, while the shape of TDS/PDS varies significantly as a function of the reciprocal space location of the corresponding Bragg reflection (Lei *et al.*, 1999, Kobas *et al.*, 2005b).

Interpreting unresolved Bragg reflections as disorder diffuse scattering means that a perfectly ordered structure is misunderstood as being disordered. Apart from this qualitative misinterpretation, quantitative structure determination is accompanied by errors, which are best understood in Patter-

son space. Two extreme cases will be compared for discussing the influence on the model obtained from such ambiguous diffraction patterns. First, it is assumed that the total scattering, *i.e.* Bragg and diffuse scattering is considered, *e.g.* by employing single crystal pair distribution function techniques (Schaub *et al.*, 2009). In this case, the influence of the resolution function can be easily understood using the convolution theorem. Convolution of the total scattering intensities with a resolution function has the effect of multiplying the Patterson densities of a perfect crystal with the Fourier transform of the resolution function. In the examples shown above, the Fourier transforms of the resolution functions are Gaussians with half-widths of several hundred Ångströms. As the maxima of the Gaussians are at the origin of the Patterson space, information about closely neighbouring atoms is almost unaffected by resolution effects, while correlations between atoms become more and more damped with increasing distance. In other words, short and medium range features of the structure can be fully revealed with the total scattering approach, even if the artificial diffuse scattering is misinterpreted as disorder diffuse scattering.

On the other hand, if structure analysis is exclusively based on visible Bragg scattering without considering artificial diffuse intensities, information about *broad* diffraction features is missed, which leads to artefacts at *short* distances in Patterson space. Any structure determination based on Bragg reflections alone must therefore be incomplete regarding the description of short inter-atomic distances and thus essential information about crystal-chemical building principles of the structure is lost. The effect of ignoring the artificial diffuse scattering is similar to using only strong reflections in the structure determination of quasicrystals. Corresponding consequences were discussed by Ma *et al.* (1989) and Lei *et al.* (1991) and it was shown that Patterson maps calculated from strong reflections only, show significant artefacts at short distances.

3. Examples

3.1 Diffuse scattering from $d\text{-Al}_{70}\text{Co}_{12}\text{Ni}_{18}$

Figure 2 shows sections from the zeroth layer of the compound $d\text{-Al}_{70}\text{Co}_{12}\text{Ni}_{18}$ at room temperature and at 1070 K. The experiment was done at the Swiss-Norwegian beamline at the synchrotron facility ESRF, Grenoble, France using a MAR345 image plate detector (for further experimental details and for a more comprehensive overview over the reciprocal space of this compound see Steurer *et al.*, 2001). The room temperature pattern (Fig. 2b) shows quite a dense set of Bragg peaks. The shortest observable separation between Bragg reflections is small ($\sim 0.005 \text{ \AA}^{-1}$), *i.e.* about 2.5 times the FWHM ($\sim 0.002 \text{ \AA}^{-1}$). The next shorter separation between Bragg reflections would be expected to be $\sim 0.005 \text{ \AA}^{-1}/\tau \approx 0.003 \text{ \AA}^{-1}$, which is close to the half-width of the resolution function. If present, such reflections and reflections having even shorter distances would not be resolved (see chapter 2), but contribute to the diffuse intensities. It can therefore not be discounted that at least a part of the diffuse intensities shown in Fig. 2b represents unresolved

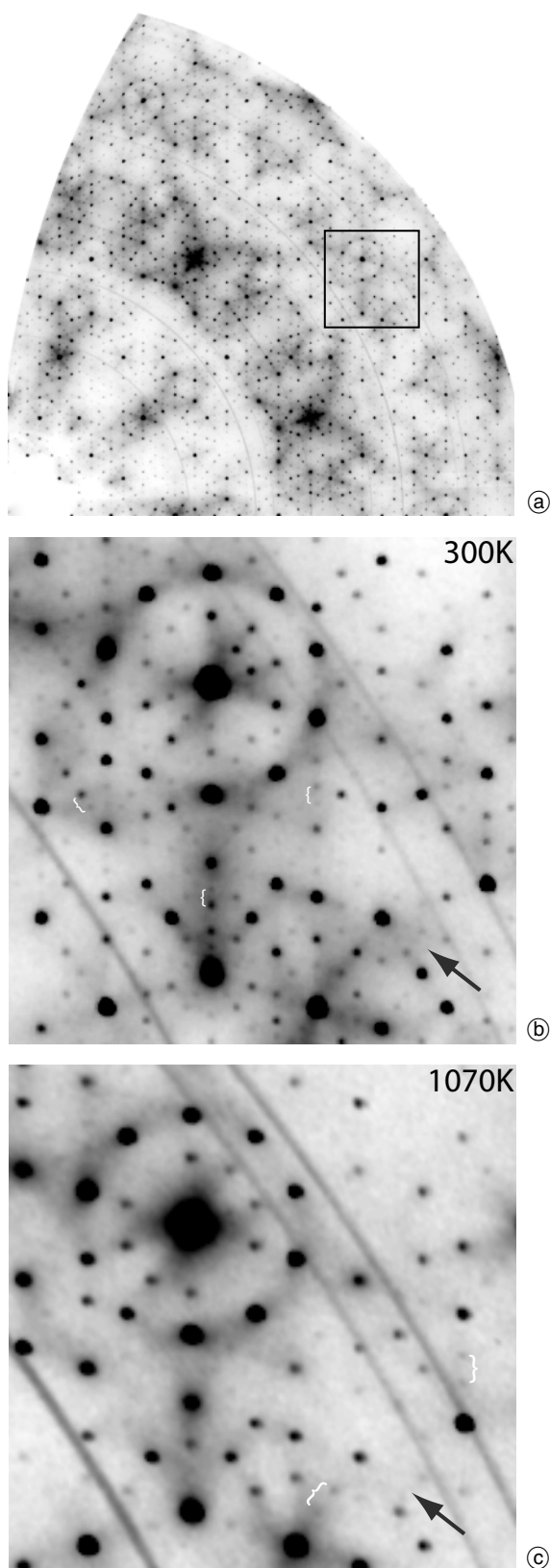


Fig. 2. Diffraction patterns from the zeroth layer of the compound $d\text{-Al}_{70}\text{Co}_{12}\text{Ni}_{18}$ at room temperature (**a**, **b**) and 1070 K (**c**). The sections (**b**) and (**c**) cover a range from 0.5 to 0.65 \AA^{-1} along the x direction and from 0.3 to 0.45 \AA^{-1} along y (all in cartesian coordinates). The position of the sections in a more complete diffraction pattern is indicated by a square in (**a**). The braces show examples for the shortest observable distance between two reflections and the arrows indicate diffuse scattering that is significantly weaker at 1070 K compared to the room temperature pattern. The powder rings are coming from the sample holder.

Bragg reflections. When comparing the room temperature pattern with the 1070 K intensities (Fig. 2c) the origin of the diffuse scattering becomes clearer. Room and high temperature diffraction patterns are very similar, but at 1070 K the density of observable Bragg reflections is significantly smaller than at room temperature. Reflections having a separation of $\sim 0.005 \text{ \AA}^{-1}$ are not visible at all, and ones separated by 0.008 \AA^{-1} are weak and rare. The Bragg reflections are slightly broader at 1070 K (FWHM $\approx 0.003 \text{ \AA}^{-1}$), which may be due to structural effects, but small changes in the experimental setup may also be responsible (the needle-like crystal has moved between the measurements, what may influence the shape and the width of the resolution function). The increased experimental width of the reflections cannot be fully responsible for the observations. At the given conditions, it would be expected that at least reflections having a separation of $\sim 0.008 \text{ \AA}^{-1}$ are hardly affected by resolution effects. Therefore, structural changes, which are most probably temperature induced phasonic distortions, must be the reason for the smaller density of observable reflections. An important conclusion can be drawn from the observations. Phasonic disorder also weakens potentially unresolved Bragg reflections, as they are expected to have very high perpendicular space components. Therefore, it can be assumed that unresolved Bragg reflections are absent at high temperatures and that diffuse scattering is only coming from disorder. When comparing the patterns in Figs. 2b and c, one finds that high temperature diffuse scattering indeed becomes weaker at some regions (see arrows), and stronger at other places. The major part of reciprocal space, however, shows no significant changes and therefore most of the diffuse scattering seen at room temperature must be coming from disorder. The observation of decreasing diffuse intensities at some parts of the high temperature pattern may be seen as a hint for contributions of unresolved Bragg reflections at room temperature, but alternative explanations cannot be excluded *a-priori*. A final proof for the presence of unresolved Bragg reflections at room temperature can only be given if the experiment is repeated with higher resolution. Significant influence from truncation effects to the appearance of the diffuse pattern can be excluded since the butterfly-like shape of the diffuse scattering close to strong Bragg reflections is typical for TDS/PDS and furthermore, appearance of the diffuse scattering strongly varies as a function of the reciprocal space position of the associated Bragg reflections.

3.2 Diffuse scattering from $i\text{-Al}_{64}\text{Cu}_{23}\text{Fe}_{13}$

The aim of the diffraction experiment with $i\text{-Al}_{64}\text{Cu}_{23}\text{Fe}_{13}$ was testing how dense observable Bragg reflections may get, if experimental conditions are highly optimized for measuring weak intensities. To answer this question an experiment was done at the beamline X06SA at Swiss Light Source (SLS), Villigen, Switzerland using the PILATUS 6M pixel detector (Kraft *et al.*, 2008). A detailed description of the experiment is found in Weber *et al.* (2008). The detector is free of intrinsic noise, it provides energy discrimination for suppressing fluorescence scatter-

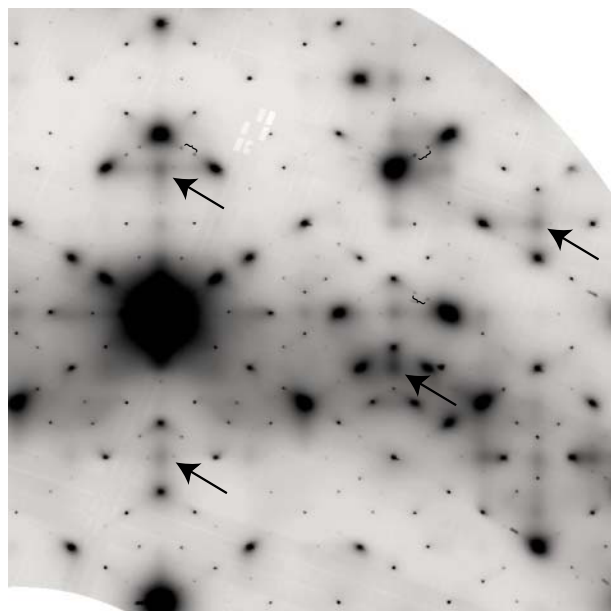


Fig. 3. Section from the zeroth two-fold layer of $i\text{-Al}_{64}\text{Cu}_{23}\text{Fe}_{13}$. The section covers a range from -0.1 \AA^{-1} to 0.3 \AA^{-1} along the x direction and from 0.3 to 0.7 \AA^{-1} along the y -direction (all in cartesian coordinates). The arrows indicate diffuse maxima at positions that are expected to be extinct due to the F -centered Bravais lattice. The braces show examples for the smallest observable distance between two Bragg reflections.

ing and it has practically no readout dead time. These detector properties allowed an experimental strategy that was not feasible before: ϕ -scans over 10° with a fine slicing of 0.1° per frame were repeated 753 times and averaged. The result is a high-resolution pattern, which has an extraordinary large dynamic range of almost 10^9 (Fig. 3). The shortest observed separation between Bragg reflections is 0.01 \AA^{-1} , while the FWHM of Bragg peaks is about 0.001 \AA^{-1} . In analogy to the high temperature diffraction pattern discussed in chapter 3.1, and given that the shortest observable separation is 0.01 \AA^{-1} , we can conclude that it is very unlikely that Bragg reflections of significant intensity are present having a separation smaller than the resolution limit of $\sim 2 \times \text{FWHM}_{\text{Bragg}} = 0.002 \text{ \AA}^{-1}$. Bragg reflections can therefore not be considered as forming a dense set and consequently, unresolved Bragg reflections do not significantly contribute to the diffuse intensities. Two different diffuse features are observable in the diffraction pattern. Relatively strong features are found beneath Bragg reflections with high intensity. Shape and intensity distribution is typical for TDS and PDS and may be interpreted accordingly, although some contributions from truncation effects at positions showing strong TDS/PDS cannot be excluded. The second kind of diffuse scattering phenomena found in the pattern are weak maxima, which are not accompanied by Bragg reflections (see arrows in Fig. 3). The maxima are at Bragg positions that are expected to be extinct due to the average 6D F -centred Bravais lattice. The diffuse peaks indicate that higher-dimensional F -centering is fulfilled on average only, while on a local scale occupation domains separated by Bravais vectors $(\frac{1}{2} \frac{1}{2} 0 0 0 0)$ etc., are not identical. For a more detailed discussion about order and disorder in this compound, see Weber *et al.* (2008).

4. Discussion and conclusion

As demonstrated by the examples in chapter 2, presence of diffuse scattering in the diffraction pattern of quasicrystals is not a proof for the presence of disorder. Even in the case of perfect quasicrystals, limited experimental resolution may lead to visible or even strong artificial diffuse scattering. For the understanding of a crystal structure and in particular for answering the question whether a quasicrystal is perfectly ordered or not, it is essential to distinguish artificial continuous scattering from disorder diffuse scattering. Some criteria are given in the following:

- TDS/PDS can be easily distinguished from truncation effects by analysing the reciprocal space behaviour of the diffuse intensities as discussed in chapter 2.
- Diffuse scattering is not expected to come from unresolved Bragg peaks, if the smallest observable separation between Bragg reflections is significantly larger than the FWHM of the resolution function (see examples in chapter 3).
- In the case that Bragg reflections are closer than about two or three half-widths of the resolution function, contributions of unresolved Bragg intensities to the diffuse pattern must be considered. Improvement of reciprocal space resolution or temperature dependent measurements (*cf.* chapter 3.1), may help to identify the degree of resolution effects.
- Observation of time dependent intensity fluctuations in coherent diffraction experiments (Létoublon *et al.*, 2001; Francoual *et al.*, 2003) is a proof for the presence of dynamic disorder.
- Diffuse maxima may be interpreted as resulting from disorder, if a (sub-)set of the diffuse pattern is systematically free of Bragg scattering. Examples include the well-known, completely diffuse inter-layers in decagonal systems, which correspond to a short-range ordered superstructure along the periodic direction, or diffuse maxima at positions of systematically absent Bragg reflections (see chapter 3.2).
- Quasicrystals having periodic directions may show artificial diffuse scattering as discussed in this paper exclusively within the aperiodic subspace (*e.g.* ten-fold layers in decagonal quasicrystals). Any diffuse feature showing significant extensions along periodic directions can therefore not be coming from unresolved Bragg reflections. The reverse conclusion is not true. A diffuse feature that is strictly confined to the aperiodic subspace may either come from unresolved Bragg peaks or from disorder that is only present along aperiodic directions (*e.g.* phasonic disorder, short-range ordered aperiodic superstructures *etc.*).
- Disorder may further be identified using complementary methods, *e.g.* electron microscopy (Abe *et al.*, 2003).

Unresolved Bragg reflections are not only a problem in diffraction experiments with quasicrystals, but well known *e.g.* in powder diffraction experiments, where a 3D reciprocal lattice is projected to a 1D pattern. What can we learn from the experience of the powder diffraction com-

munity regarding the handling of unresolved reflections? From the experimental point of view it is clear that optimized reciprocal space resolution and reduced parasitic background are essential for a successful structure determination of quasicrystals. If experimental limits cannot be pushed further, powder diffraction inspired data evaluation techniques might allow getting better results from unresolved experimental data. The most popular technique used in powder crystallography is full-profile Rietveld refinement. If extended to three-dimensional space using single crystal diffraction data, not only integral Bragg intensities but also experimental factors like peak shape, background, *etc.* would be determined at the same time. Such three-dimensional full-profile refinements would certainly improve the interpretability of unresolved features. Currently, however, single crystal Rietveld refinement of quasicrystals is not feasible. Algorithms are not yet developed and computational requirements for fitting diffraction patterns of complex five- or six-dimensional quasicrystal structures to many gigabytes of experimental data are beyond current possibilities. A more promising approach to be adopted from powder diffraction techniques is the generalization of the pair distribution function method to single crystal diffraction data. Including diffuse scattering simply by analyzing the Fourier transform of the total diffraction pattern is expected to provide a better understanding of local properties of a structure. The development of the single crystal pair distribution function method is in progress and its usefulness has been demonstrated for quasicrystals (Kobas *et al.*, 2005a; Schaub *et al.*, 2009) and for disordered periodic structures (Schaub *et al.*, 2007).

References

- Abe, E.; Pennycook S. J.; Tsai, A. P.: Direct observation of a local thermal vibration anomaly in a quasicrystal. *Nature* **421** (2003) 347–350.
- Francoeur, S.; Livet, F.; de Boissieu, M.; Yakhov, F.; Brey, F.; Létoublon, A.; Caudron, R.; Gastaldi, J.: Dynamics of phason fluctuations in the *i*-AlPdMn quasicrystal. *Phys. Rev. Lett.* **91** (2003) 225501.
- Kobas, M.; Weber, T.; Steurer, W.: Structural disorder in the decagonal Al–Co–Ni. I. Patterson analysis of diffuse X-ray scattering data. *Phys. Rev. B* **71** (2005a) 224205.
- Kobas, M.; Weber, T.; Steurer, W.: Structural disorder in the decagonal Al–Co–Ni. II. Modeling. *Phys. Rev. B* **71** (2005b) 224206.
- Kraft, P.; Henrich, B.; Eikenberry, E.F.; Broennimann, C.; J. Synchrotron Radiat. **15** (2008) *in preparation*.
- Lei, J.; Wang, R.; Hu, C.; Ding, D. H.: Diffuse scattering from decagonal quasicrystals. *Phys. Rev. B* **59** (1999) 822–828.
- Létoublon, A.; Yakhov, F.; Livet, F.; Bley, F.; de Boissieu, M.; Mancini, L.; Caudron, R.; Vettier, C.; Gastaldi, J.: Coherent x-ray diffraction and phason fluctuations in quasicrystals. *Europhys. Lett.* **54** (2001) 753–759.
- Li, X.; Stern, A.E.; Ma, Y.: Requirements for structure determination of aperiodic crystals. *Phys. Rev. B* **43** (1991) 1371–1377.
- Ma, Y.; Stern, M.A.; Li, X.; Janot, J.: Patterson analysis of aperiodic crystals. *Phys. Rev. B* **40** (1989) 8053–8056.
- Schaub, P.; Weber, T.; Steurer, W.: Exploring local disorder in single crystals by means of the three-dimensional pair distribution function. *Philos. Mag.* **87** (2007) 2781–2787.
- Schaub, P.; Weber, T.; Steurer, W.: (2009) *in preparation*.
- Steurer, W.; Cervellino, A.; Lemster, K.; Ortelli, S.; Estermann M. A.: Ordering principles in decagonal Al–Co–Ni quasicrystals. *Chimia* **55** (2001) 528–533.
- Weber, T.; Deloudi, S.; Kobas, M.; Yokoyama, Y.; Inoue, A.; Steurer, W.: Reciprocal-space imaging of a real quasicrystal. A feasibility study with PILATUS 6M. *J. Appl. Crystallogr.* **41** (2008) 669–674.